Fish and Shellfish Immunology 87 (2019) 778–787

Contents lists available at ScienceDirect

Fish and Shellfish Immunology

journal homepage: www.elsevier.com/locate/fsi

Full length article

Dual RNA-Seq reveals the role of a transcriptional regulator gene in pathogen-host interactions between *Pseudomonas plecoglossicida* and *Epinephelus coioides*

Beibei Zhang[a,b], Zhixia Zhuang[a], Xiaoru Wang[a], Huabin Huang[a], Qi Fu[a], Qingpi Yan[b,*]

[a] College of Environment and Public Health, Xiamen Huaxia University, Xiamen, Fujian, 361024, China
[b] Fisheries College, Key Laboratory of Healthy Mariculture for the East China Sea, Ministry of Agriculture, Jimei University, Xiamen, Fujian, 361021, China

ARTICLE INFO

Keywords:
Immune response
Epinephelus coioides
Pseudomonas plecoglossicida
Transcriptional regulator gene
RK21_RS10315
RNAi
RNA-Seq

ABSTRACT

Pseudomonas plecoglossicida is a highly pathogenic bacterium for maricultured fish and causes serious losses. A transcriptional regulator gene *RK21_RS10315* was found up-regulated during the whole infection process, which was confirmed by qRT-PCR. Five shRNA were designed to silence *RK21_RS10315* gene, and the gene expression was reduced up to 96.1%. Compared with the counterpart infected with wild type strain, the infection of *RK21_RS10315*-RNAi strain resulted in the death time delay, and 90% reduction in mortality of *Epinephelus coioides*, as well as the alleviation in the symptoms of *E. coioides* spleen. Moreover, compared with the fish infected with wild type strain, the infection of *RK21_RS10315*-RNAi strain of *P. plecoglossicida* resulted in a significant change both in transcriptome of spleen of infected *E. coioides* and *P. plecoglossicida*. The KEGG analysis showed that genes of 16 immune pathways in *E. coioides* were affected by the silence of *RK21_RS10315* of *P. plecoglossicida*. Among them, intestinal immune network for IgA production pathway and leukocyte transendothelial migration pathway were more prominent than other pathways. 19 euk-DEMs in these immune pathways had varying degrees of correlation with 19 pro-DEMs, and the expression of *ipxA*, *grpE*, *yhbJ*, *truD* and *suhB* from 19 pro-DEMs were predicted more related to *RK21_RS10315* in *P. plecoglossicida*.

1. Introduction

The infection process is a fierce battle between the pathogen and the host, in which both the pathogen and the host must do their best to win [1]. In order to win this life-and-death struggle, both the pathogen and the host must mobilize all available resources, and all changes will be reflected in their respective transcriptome profiles [2]. Thus, the simultaneous monitoring of the RNA expression profiles of the two interacting species during infection is important to obtain a comprehensive understanding of the pathogenic mechanisms and the host immune response [3]. RNA-Seq is a sensitive tool used to study global gene expression of the host or pathogen during infection and has identified many important functional genes [4,5]. To gain a better understanding of host-pathogen interactions, dual RNA-Seq was introduced to simultaneously profile host and pathogen transcriptomes for the first time in 2012 [4]. Recently, dual RNA-Seq analyses were performed successfully in *Salmonella typhimurium* with HeLa cells [5] and *Streptococcus pneumonia* with lung epithelial cells to assess pathogen-host interactions [6]. However, studies on the use of dual RNA-Seq to explore the function of certain genes in pathogen-host interactions have not been reported.

Pseudomonas plecoglossicida is one of the most important pathogens associated with the fulminating infectious disease of large yellow croaker (*Pseudosciaena crocea*) [7] and *Epinephelus coioides* [8]. The visceral white spot disease caused by *P. plecoglossicida* is known for its high morbidity and mortality, and this disease causes direct economic losses of more than one hundred million yuan each year [7]. To reveal the pathogen-host interactions between *P. plecoglossicida* and *E. coioides* in depth, dual RNA-Seq was performed to monitor the transcriptome profiles of *P. plecoglossicida* and *E. coioides* during infection (unpublished results), and the data have been deposited in the NCBI Sequence Read Archive (SRA) under the accession number SRP115064. The data showed that the expression of the *RK21_RS10315* gene of *P. plecoglossicida* was significantly expressed throughout the entire infection process. Therefore, *RK21_RS10315* was hypothesized to play a role in the pathogenicity of *P. plecoglossicida*.

The protein encoded by the *RK21_RS10315* gene was annotated as a sigma-54-dependent Fis family transcriptional regulator (reference:

* Corresponding author.
E-mail address: yanqp@jmu.edu.cn (Q. Yan).

https://doi.org/10.1016/j.fsi.2019.02.025
Received 12 December 2018; Received in revised form 26 January 2019; Accepted 15 February 2019
Available online 16 February 2019

accession number SRP115064). These transcriptional regulators typically contain three domains, the N-terminal regulatory (R) domain, the central AAA + domain (C), and the C-terminal DNA binding domain (D), while the sigma54 family has only one member [9], and its transcriptional regulatory activity relies on an activator that hydrolyses ATP to generate energy to initiate closed complex (CC) isomerization of the holoenzyme complex (RNAP-sigma54) and initiate transcription [10]. It has become clear that these proteins are central to the function of the RNA polymerase holoenzyme from the results of previous research [11]. The bacterial sigma-54-RNA polymerase is used in sophisticated signal transduction pathways [12] involving transcriptional activation via remote enhancer elements [13–15]. With the recognition that the sigma-54 protein was once regarded as an aspect of transcription restricted to higher organisms, it has become a well-established feature of certain bacterial regulatory systems, particularly those associated with nitrogen metabolism [16–18]. Therefore, we suspect that the *RK21_RS10315* gene may play a role in pathogen-host interactions. However, until now, no study has reported on the role of *RK21_RS10315* during *E. coioides* infection by *P. plecoglossicida*.

Considering the economic impact of the high mortality of cultured *E. coioides* caused by *P. plecoglossicida* and the potential significant role of *RK21_RS10315* in the virulence of *P. plecoglossicida*, the *RK21_RS10315* gene of *P. plecoglossicida* was silenced by RNAi. Subsequently, the virulence to *E. coioides* of the wild-type and *RK21_RS10315*-RNAi-silenced *P. plecoglossicida* strains was compared. The spleens of *E. coioides* infected with the wild-type and *RK21_RS10315*-RNAi-silenced *P. plecoglossicida* strains were subjected to dual RNA-Seq. The purpose of this study was to elucidate the immune response of *E. coioides* with respect to the *RK21_RS10315* gene of *P. plecoglossicida* by dual RNA-Seq.

2. Materials and methods

2.1. Bacterial strains and culture conditions

A highly pathogenic *P. plecoglossicida* strain (NZBD9) was isolated from a naturally infected large yellow croaker and was confirmed to be pathogenic by artificial infection [7]. The *P. plecoglossicida* strain was routinely grown in Luria-Bertani (LB) broth or on LB agar solidified medium at 18 °C with shaking at 220 rpm. *Escherichia coli* DH5α was obtained from TransGen Biotech (Beijing, China) and was cultured in LB medium (37 °C, 220 rpm).

2.2. Construction of P. plecoglossicida RNAi strains

RNAi strains were constructed according to methods described by Zhang et al. [2]. Invitrogen Block-iT RNAi Designer (http://rnaidesigner.thermofisher.com/rnaiexpress/setOption.do?designOption=shrna&pid=7085871032206845) was used to predict shRNA sequences that would silence the *RK21_RS10315* genes. Five short hairpin RNA sequences targeting the *RK21_RS10315* genes were designed and synthetized (Table S1). After linearizing pCM130/tac vectors with the restriction enzymes *Nsi*I (R3127S) and *BsrG*I (R3575S) (New England Biolabs, including TIME-SAVER™ Protocol and Buffer Performance), the oligonucleotides were annealed and ligated to the linearized pCM130/tac vectors using T4 DNA ligase (New England Biolabs) following the manufacturer's recommendations. The recombinant pCM130/tac vectors were transformed into the competent *E. coli* DH5a cells (*Trans5α* Chemically Competent Cells) by heat shock and then were electroporated into *P. plecoglossicida* as described previously [19]. Finally, the expression level of *RK21_RS10315* in each RNAi strain was detected by qRT-PCR.

2.3. Artificial infection and sampling

All animal experiments described in this study were approved by the Animal Ethics Committee of Jimei University (JMULAC201159). The Experimental Animal Care and Use Guidelines from Ministry of Science and Technology of China (MOST-2011-02) were strictly followed.

Healthy *E. coioides* (body length 14 ± 2 cm) were obtained from Zhangzhou (Fujian, China) and acclimatized at 18 °C for one week under specific pathogen-free laboratory conditions. For survival assays, 30 fish were randomly divided into three groups, each group were injected with 10^3 *cfu/g* wild strain of *P. plecoglossicida*, RNAi strain of *P. plecoglossicida* and saline respectively. The water temperature during infection was maintained at 18 ± 1 °C. The status of the fish was recorded three times a day. For tissue RNA-Seq, the spleens of six *E. coioides* infected with the wild-type or RNAi *P. plecoglossicida* strain were sampled at 48 h post infection (hpi). Every two spleens were mixed as one sample. For the tissue distribution assays, the spleens, livers, head kidneys, trunk kidneys and blood of three infected *E. coioides* were sampled at 6, 12, 24, 48, 72, 96 and 120 hpi [20].

2.4. DNA isolation

DNA from spleens, livers, head kidneys and trunk kidneys was purified with an EasyPure Marine Animal Genomic DNA Kit (TransGen Biotech, Beijing, China) following the manufacturer's instructions. The EasyPure Blood Genomic DNA Kit (TransGen Biotech) was used for DNA isolation from blood samples.

2.5. RNA isolation and reverse transcription

Total RNA was extracted using TRIzol reagent (Invitrogen, Carlsbad, CA, USA) according to the manufacturer's instructions. The mixed genomic DNA in total RNA was digested with the Turbo DNA-free DNase (Ambion, Austin, TX, USA). The RNA quality was assessed using an Agilent 2100 Bioanalyzer (Agilent Technologies, Santa Clara, CA, USA), while the rRNA in the total RNA was removed using a Ribo-Zero rRNA Removal Kit (Epicentre, Madison, WI, USA) according to the manufacturer's instructions. The quality of the total RNA was assessed by agarose gel electrophoresis. The cDNA was synthesized using a TaKaRa PrimeScript™ RT-PCR Kit (TaKaRa Bio Group, JAPAN). The synthesized cDNA was used as a new sample template for qRT-PCR and then was stored at −20 °C until use.

2.6. qRT-PCR

qRT-PCR was performed using a QuantStudio 6 Flex instrument (Life Technologies). All primer sequences are provided in Table S2. Reaction mixtures (10 μL/UltraFlux®i 8-strip Low Profile 0.1 mL w/individual attached Flat cap) were comprised of 5 μL qMix (Life Technologies), 0.25 μL of the forward primer, 0.25 μL of the reverse primer, 0.5 μL of diluted template DNA and 4 μL of nuclease-free water. The expression of bacterial genes was normalized using the 16S RNA gene. For *E. coioides*, the expression of mRNA was normalized to *β-actin*. The copy number of the *gyrB* gene was used to estimate *P. plecoglossicida* abundance. Three replicates were performed for each treatment, and the $2^{-\Delta\Delta Ct}$ method [21] was used to calculate the relative level of gene expression. High throughput sequencing results were confirmed by qRT-PCR (Fig. S1).

2.7. Transcriptomic analysis

2.7.1. Library preparation and sequencing

The dual RNA-Seq libraries were prepared using protocols supplied with the TruSeq™ RNA sample preparation Kit (Illumina, San Diego, CA, USA). RNA quality was determined by a 2100 Bioanalyzer (Agilent) and was quantified using a ND-2000 instrument (NanoDrop Technologies). Only a high-quality RNA sample (OD260/280 = 1.8–2.2, OD260/230 ≥ 2.0, RIN ≥ 6.5, 28S:18S ≥ 1.0, > 10 μg) was used to construct sequencing library. In brief, the rRNA-depleted

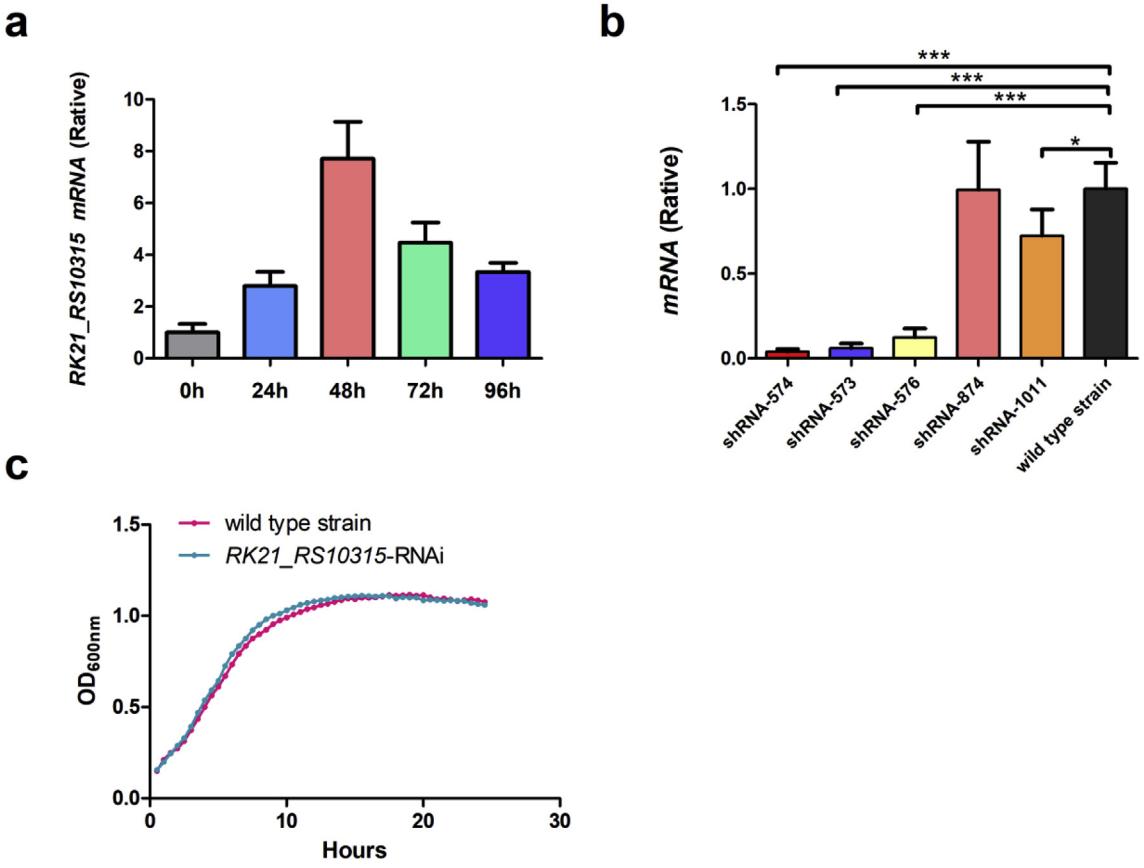

Fig. 1. Construction of the *RK21_RS10315*-RNAi strain of *P. plecoglossicida*. (a): Expression level of *RK21_RS10315* gene of wild type *P. plecoglossicida* at different infection times. (b): The mRNA expression of 5 *RK21_RS10315*-RNAi silencing strains. $^{**}P \leq 0.01$; $^{***}P \leq 0.001$. (c): Growth curve of *P. plecoglossicida*.

RNA sample was fragmented in fragmentation buffer, and cDNA synthesis was performed using a SuperScript double-stranded cDNA synthesis kit (Invitrogen, Carlsbad, CA, USA). After end reparation, phosphorylation and poly (A) addition, the cDNA library was amplified using Phusion DNA polymerase (NEB). Small RNA-Seq libraries were generated using a TruSeqTM Small RNA Sample Prep Kit (Illumina) following the manufacturer's instructions. An Agilent 2100 Bioanalyzer instrument (Agilent Technologies) was used to validate the library quality. Sequencing was performed on an Illumina HiSeq4000 sequencing platform at Majorbio Biotech Co., Ltd. (Shanghai, China).

2.7.2. Processing and mapping of reads

The trimming and quality control of raw Illumina reads were performed using Sickle (https://github.com/najoshi/sickle) and SeqPrep (https://github.com/jstjohn/SeqPrep) with the default settings [22,23]. For dual RNA-Seq, clean data were mapped to the genome of *P. plecoglossicida* strain NyZ12 (NCBI RefSeq accession number: NZ_ASJX00000000.1) using Bowtie2 [24]. Mapped reads were classified as reads of *P. plecoglossicida*, and the leftover reads were used for de novo assembly to obtain the *E. coioides* unigenes.

2.7.3. De novo assembly and annotation of mRNAs in the E. coioides transcriptome

All the clean reads that did not map to the *P. plecoglossicida* genome (NYz12) from the wild-type strain and the RNAi strain-infected spleens were treated as a pool of reads. The pool of reads was assembled de novo into unigenes using Trinity [25]. *RSEM* (http://deweylab.biostat.wisc.edu/rsem/) [26] was used to quantify gene abundances. The R statistical package software EdgeR (Empirical analysis of Digital Gene Expression in R, http://www.bioconductor.org/packages/2.12/bioc/html/edgeR.html) [27] was used for differential expression analysis. To annotate the mRNAs, the clean unigenes were compared against different databases, including the NCBI NR protein, STRING, SWISS-PROT and KEGG (Kyoto Encyclopedia of Genes and Genomes) databases using BLASTX to identify the proteins that shared the greatest sequence similarity with the identified unigenes. Finally, KEGG was used for metabolic pathway analysis (http://www.genome.jp/kegg/) [28].

2.7.4. Analysis of differential gene expression

The measurement of differentially expressed genes was performed for the *P. plecoglossicida* and *E. coioides* libraries. Expression analyses of genes from the pathogen and host were based on annotations from NCBI (NZ_CP010359.1) and the reference transcriptome annotation for the *E. coioides* samples described above, respectively. After obtaining unique mapped read counts, the R package edgeR (version 3.10.2) [27] was used to identify differentially expressed genes, which were determined using the following thresholds: $|\log 2^{\text{fold change}}| \geq 1$ as well as false discovery rate (FDR) < 0.05.

2.7.5. KEGG-enrichment analysis

All the differentially expressed mRNAs (*DEMs) of the host and pathogen* were used for the KEGG enrichment analysis. The KEGG pathway enrichment was carried out with KOBAS (KEGG Orthology-Based Annotation System) [29]. Fisher's exact test (adjusted P value ≤ 0.05) was used to analyse the differentially expressed KEGG pathways.

2.7.6. Key virulence gene prediction, construction of interaction network

Differentially expressed mRNAs from the host (eukaryotic differential genes: euk-DEMs) and the pathogen (prokaryotic differential genes: pro-DEMs) were selected to predict the key virulence genes by expression correlation analysis. Interaction networks of euk-DEMs and

the corresponding pro-DEMs were constructed using Cytoscape (http://www.cytoscape.org/).

2.7.7. Statistical analyses

All data were expressed as the means ± standard deviation (SD) from at least three sets of independent experiments. Data analysis was performed using SPSS 17.0 (Chicago, IL, USA), and one-way analysis of variance with Dunnett's test was used. P values < 0.05 were considered significant.

2.8. Data access

The RNA sequencing reads data were deposited at the GenBank SRA database under the accession numbers SRP115064 and SRP168002.

3. Results

3.1. Construction of the RK21_RS10315-RNAi strain

Fig. 1a shows the qRT-PCR results for the *RK21_RS10315* gene expression of *P. plecoglossicida* at different infection times. The data showed that *RK21_RS10315* gene of *P. plecoglossicida* were significantly high expressed after 24hpi, 48hpi, 72hpi and 96hpi compared with the bacteria of 0hpi (*in vitro*)(Fig. 1a), which was consistent with previous RNA-Seq results.

Four of the five shRNAs significantly reduced the mRNA expression of *RK21_RS10315* with different efficiencies (Fig. 1b). The strain containing pCM130/tac-*RK21_RS1*0315-shRNA-574 exhibited the best gene silencing efficiency (96.1%) and was chosen for further studies (Fig. 1b). Despite *RK21_RS10315* being silenced, the growth rates of the wild-type and *RK21_RS10315*-RNAi strains were almost the same (Fig. 1c).

3.2. Effects of RK21_RS10315 on the pathogenicity of P. plecoglossicida

Compared with *E. coioides* injected with the wild-type strain, those injected with the *RK21_RS10315*-RNAi strain exhibited a significant delay in the time of death and a significant decrease in mortality (Fig. 2a). At 72hpi, the spleens of the *E. coioides* injected with the wild-type *P. plecoglossicida* strain showed typical symptoms (the surface of the spleen was covered with numerous white spots). However, unobvious white spots were observed on the surfaces of the spleens of *E. coioides* injected with the *RK21_RS10315*-RNAi strain (Fig. 2b). The difference in the abundance of the white spots between the wild-type strain and mutant *E. coioides* strains varied with different organs at different times. Moreover, the percentage of *RK21_RS10315*-RNAi strain abundance to that of the wild-type strain increased with the time post infection. The percentage of *RK21_RS10315*-RNAi strain abundance to that of the wild-type strain in the spleen and liver was much higher than that in the head kidney and blood. At 120hpi, the abundances of the *RK21_RS10315*-RNAi strain in the spleens, trunk kidneys, blood and livers were close to those observed in the wild-type strain (Fig. 2c).

3.3. Dual RNA-Seq of spleen tissue from infected E. coioides

3.3.1. P. plecoglossicida-induced host responses

3.3.1.1. Correlation of transcriptional data. In the RNA-Seq approach with host tissue, (*i*) transcriptome data from the spleens of *E. coioides* infected with the *RK21_RS10315*-RNAi strain, (*ii*) transcriptome data from the spleens of *E. coioides* infected with the wild-type strain and (*iii*) transcriptome data from the spleens of healthy *E. coioides* without artificial infection (negative control) were systematically catalogued. The Pearson correlation coefficients (r) for the three biological replicates are shown in Fig. 3a. All the samples closely correlated with their respective replicates from the same biological sample group ($r > 0.9$).

3.3.1.2. Differently expression genes. The gene expression profile was calculated using *edgeR*, and genes exhibiting changes in expression levels that met the FDR < 0.05 and $|\log_2 FC| \geq 1$ thresholds were considered significantly differentially expressed. In total, 153,457 mRNAs were identified from the profiled transcripts of the spleens infected with the *RK21_RS10315*-RNAi strain. Compared with the spleens infected with the wild-type strain, 22,010 mRNAs from the spleens infected with the *RK21_RS10315*-RNAi strain exhibited significantly differential abundance, with 17,689 mRNAs downregulated and 4,321 mRNAs upregulated (Fig. 3b).

Genes showing significant changes in the expression levels (at least a twofold change) were considered. According to logFC, the top 50 up- and downregulated DEMs were selected and are shown in Fig. 3c. The gene with the maximal fold change in the upregulated genes was *c177827_g2* (logFC = 10.41) and for the downregulated genes was *c154722_g1* (logFC = −6.39).

According to KEGG database, most of the DEMs were enriched in 16 KEGG immune-related pathways. Compared with the spleens infected with the wild-type strain, all of these 16 pathways were altered in spleens infected with the *RK21_RS10315*-RNAi strain. (Fig. 4). According to the P-value of Fisher's exact test, ko04672, which represents intestinal immune network for IgA production, was significant. In addition, ko04670, a pathway of leukocyte transendothelial migration, had the most differentially expressed genes and had a higher ratio than the other pathways.

In the intestinal immune network for the IgA production pathway, genes encoding IL10, TACI, LTβR, IL15, CCR9, and CXCL12 were upregulated (Fig. 5a). There were no downregulated genes enriched in this pathway. In the leukocyte transendothelial migration pathway, genes encoding MMPs, p38, MLC, SDF-1, and RhoH were upregulated, whereas genes encoding VAV3, PTK2B, PIK3CA, VCAM1 and AF-6 were downregulated (Fig. 5b). There were both down- and upregulated genes enriched in this pathway.

3.3.2. The host-responsive mRNA repertoire of P. plecoglossicidais

3.3.2.1. Correlation of transcriptional data. In the pathogenic tissue RNA-Seq approach, (*i*) transcriptome data from the spleens of *E. coioides* infected with the *RK21_RS10315*-RNAi strain, (*ii*) transcriptome data from the spleens of *E. coioides* infected with the wild-type strain and (*iii*) and transcriptome data from the wild-type strain cultivated *in vitro* (negative control) were used. The Pearson correlation coefficients (r) for the three biological replicates are indicated in Fig. 6a. All the samples closely correlated with their respective replicates from the same biological sample group ($r > 0.9$).

3.3.2.2. Differently expressed genes. The gene expression profile was calculated using *edgeR*, and the changes in the expression levels that met the FDR < 0.05 and $|\log_2 FC| \geq 1$ thresholds were considered significantly differentially expressed. In total, 5,843 mRNAs were identified from the profiled transcripts of the spleens infected with the *RK21_RS10315*-RNAi strain. Compared with the spleens infected with the wild-type strain, 65 mRNAs from the spleens infected with the *RK21_RS10315*-RNAi strain were significantly different in abundance, with 15 mRNAs downregulated and 50 mRNAs upregulated (Fig. 6b).

Genes showing significant changes in expression (at least a twofold change) were considered. According to $\log_2 FC$, all up- and downregulated DEMs were selected and are shown in Fig. 6c. The maximum differences in gene fold change were the upregulated gene *mdtB* (logFC = 15.62) and the downregulated gene rna30 (logFC = −4.4).

3.4. Coexpression analysis of differentially expressed genes among the pathogen and host

According to the p value of genes interacting with each other, 19

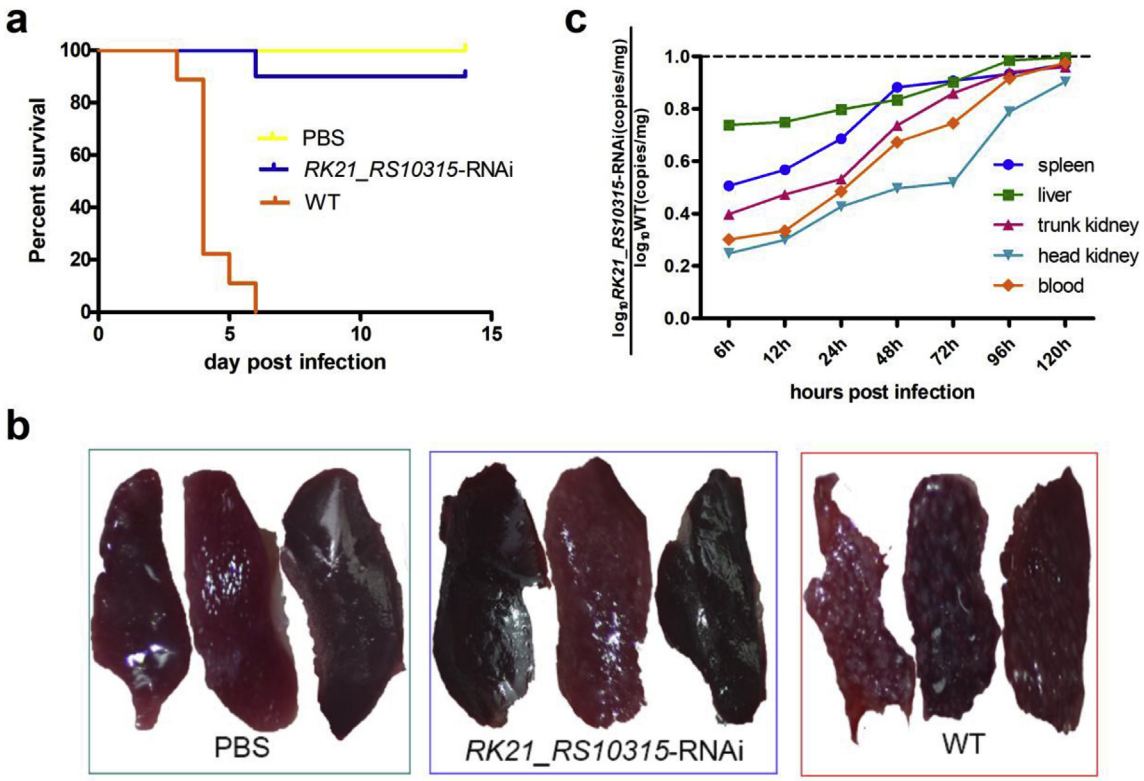

Fig. 2. The virulence of *P. plecoglossicida* towards *E. coioides*. (a): Survival rate of *E. coioides* infected by *P. plecoglossicida*. (b): Symptoms of the spleens of *E. coioides* infected with the wild-type and *RK21_RS10315*-RNAi *P. plecoglossicida* strains. (c): Spatial and temporal relative distribution of the *RK21_RS10315*-RNAi *P. plecoglossicida* strain compared to that of the wild-type strain.

genes (p value < 0.05) from Figs. 6c and 19 genes (p value < 0.05) from the important immune-related pathways were selected and are shown in Fig. 7. In Fig. 7, the host differentially expressed genes are represented by a circle, and the pathogen differentially expressed genes are represented by an inverted triangle. The redder the colour is, the greater the number of genes that were associated. The more genes that were associated with the node, the more important the potential roles in the network. As shown in Fig. 7, *ipxA* (degree = 16), *grpE* (degree = 15), *yhbJ* (degree = 15), *truD* (degree = 14) and *suhB* (degree = 13) from the pathogen DEMs were associated with the greatest number of genes from the host DEMs.

4. Discussion

Numerous genes are involved in the regulation of virulence in pathogens by regulating toxicity and invasiveness [30]. To date, numerous genes have been shown to have the ability to be associated with disease in aquatic pathogenic bacteria that are regulated, such as *sigX* in *P. plecoglossicida* [1]; *L321_RS19110* in *P. plecoglossicida* [2]; *flrA, flrB,* and *flrC* [19]; *flgE* in *Aeromonas hydrophila* [31]; *secA, secD, secF, yajC,* and *yidC* [32] and *oppABCDF* in *V. alginolyticus* [33]. However, no studies have investigated the contribution of the *P. plecoglossicida* gene *RK21_RS10315* with respect to virulence.

Gene knockout is widely used in the studies on functional genes [34–36]. RNAi is a highly efficient and specific tool for gene function study [37,38] other than knockout technology. Knocking down of key virulence genes will significantly reduce the virulence of pathogens [39,40], this advantage can be applied in vaccine development [41–43]. In the present study, 5 shRNAs were designed for 5 different targets of *RK21_RS10315*. All of the 5 shRNAs significantly reduced the *RK21_RS*10315 mRNA content, with the best gene silencing efficiency exhibiting a reduction of 96.1%. Therefore, the stable silencing technology in the present study laid the foundation for the subsequent research.

Gene expression levels are dynamically are dysregulated at different stages of the pathogen infecting the host [44]. The expression of *RK21_RS10315* in *P. plecoglossicida* was significantly higher at 48hpi than at 0hpi, indicating that *RK21_RS10315* may be involved in the regulation of virulence in *P. plecoglossicida*. Compared with infection by the wild-type strain, infection by the *RK21_RS10315*-RNAi strain alleviated the symptoms for the *E. coioides* spleen and caused an onset time delay, and a 90% reduction in *E. coioides* mortality was even observed. The results suggested that silencing *RK21_RS10315* led to a decrease in the virulence of *P. plecoglossicida*. Compared with infection with the wild-type strain, infection with the *RK21_RS10315*-RNAi strain caused significantly different symptoms in the *E. coioides* spleens. Notably, the *E. coioides* spleen is the target organ of *P. plecoglossicida* [7], suggesting that the *E. coioides* spleen is a good target to study the immune response of *E. coioides* in response to *P. plecoglossicida* infection.

Infections caused by pathogens are well known to potentially cause great changes in both the host and pathogen transcriptomes [3]. Recently, the change in a single virulence gene has been shown to cause significant changes in transcriptome responses [1,2]. In the present study, compared with the wild-type strain, the gene silencing of *RK21_RS10315* in *P. plecoglossicida* resulted in a significant change in the transcriptomes of both the infected spleen and the invading *P. plecoglossicida*. There were 22,010 and 65 differently expressed mRNAs in the infected spleen and invading *P. plecoglossicida*, respectively. The results indicated that the *RK21_RS10315* gene of *P. plecoglossicida* has an important effect when invading *E. coioides*. The results of the KEGG analysis of the infected spleens showed that 16 immune-related pathways were significantly enriched. The intestinal immune network for the IgA production and leukocyte transendothelial migration pathways were more prominent, as shown in Fig. 4. The IgA generated in the intestinal network is the first line of defence against bacteria invasion [1,45]. The intestinal immune network for the IgA production pathway

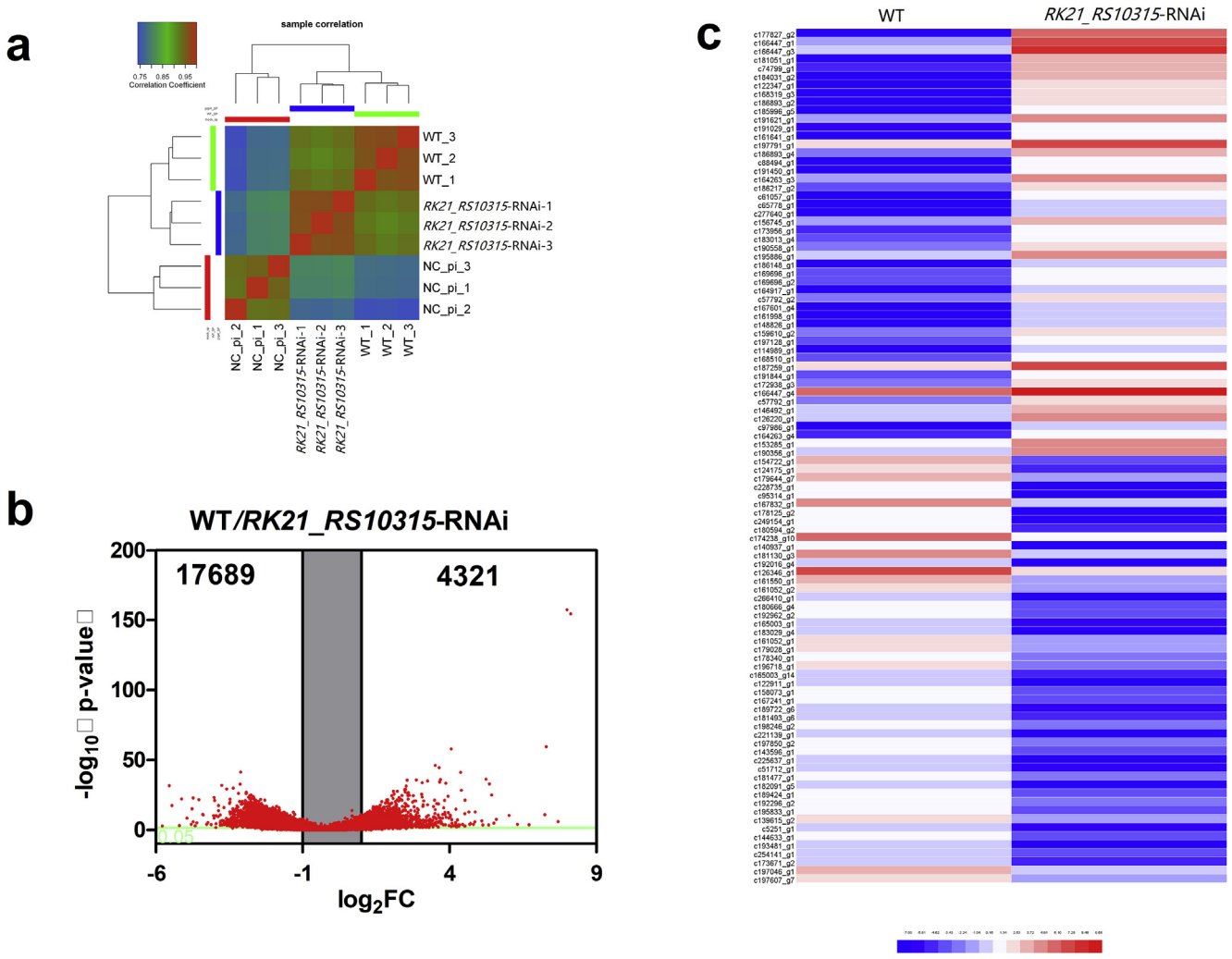

Fig. 3. Comparative transcriptional analysis of the host for *E. coioides* spleens. (a): Reproducibility of transcriptional data (Pearson correlation coefficient (r) > 0.9). (b): Volcano plot obtained from *edgeR* analysis of infected *E. coioides* RNA pools. (c): Heat map of the top 50 up- and downregulated genes from host transcripts (FDR < 0.05, | $\log_2$FC | ≥1). Colour-coding is based on $\log_2$FPKM (per kilobase of exon model per million mapped reads). (For interpretation of the references to colour in this figure legend, the reader is referred to the Web version of this article.)

has been associated with ITGAM-ITGAX, VAV3 and CARD9 and two new independent signals (HLA-DQB1 and DEFA) with the risk of inflammatory bowel disease (IBD) or maintenance of the intestinal epithelial barrier and response to mucosal pathogens, suggesting a possible role for host-intestinal pathogen interactions in shaping the genetic landscape of IgAN [46–48]. The leukocyte transendothelial migration pathway has been associated with many of the same molecules and mechanisms that regulate paracellular migration and controls transcellular migration [49]. ICAM-1-mediated and Src- and Pyk2-dependent vascular endothelial cadherin tyrosine phosphorylation and PECAM-1 are required for leukocyte transendothelial migration [50,51]. Transmigrating leukocytes undergo dramatic changes in cell shape and adhesive properties in response to inflammatory signals [52]. Although there have been reports regarding the response of these pathways to bacterial infection, the response of these pathways to a single gene during bacterial infection has not been reported. These prominent pathways in the spleens infected with the *RK21_RS10315*-RNAi strain indicated that *E. coioides* was more likely to remove the *RK21_RS10315*-RNAi strain than the wild-type *P. plecoglossicida* strain.

Organisms constantly come into physical contact with other species, resulting in changes at the molecular level, such as in the transcriptome [53]. Faced with pathogen invasion, the host has to mobilize a series of immune mechanisms to resist the pathogen [54]. In the present study, the results showed that 2 immune pathways prominently changed in response to invasion by the *RK21_RS10315*-RNAi strain, and 19 euk-DEMs in these immune pathways had varying degrees of correlation with 19 pro-DEMs. When the host defends against pathogens, the immune pathways cooperates with each other [55]. These pathways were altered in spleens of infected *E. coioides*, which was caused by the lack of *RK21_RS10315* in *P. plecoglossicida*. The differences in these pathways in the spleens infected with the *RK21_RS10315*-RNAi strain indicated that *E. coioides* was more likely to kill the *RK21_RS10315*-RNAi strain than the wild-type *P. plecoglossicida* strain. These results also partly explained why the *RK21_RS10315*-RNAi strain was less virulent and less abundant in *E. coioides*.

In conclusion, *RK21_RS10315* is a pathogenic gene of *P. plecoglossicida* that contributes to the pathogenicity of this organism against *E. coioides*. Compared to the wild-type strain, the infection of *E. coioides* with the *RK21_RS10315*-RNAi strain resulted in differences in the intestinal immune network for IgA production and leukocyte transendothelial migration pathways. Among them, correlations in gene expression between euk-DEMs and pro-DEMs with respect to each other play an important role in the pathogen-host interaction. For a better understanding of the host-pathogen interaction, time-resolved dual RNA-seq and more effective methods for association analysis of host and pathogen transcriptional data will be introduced to our further

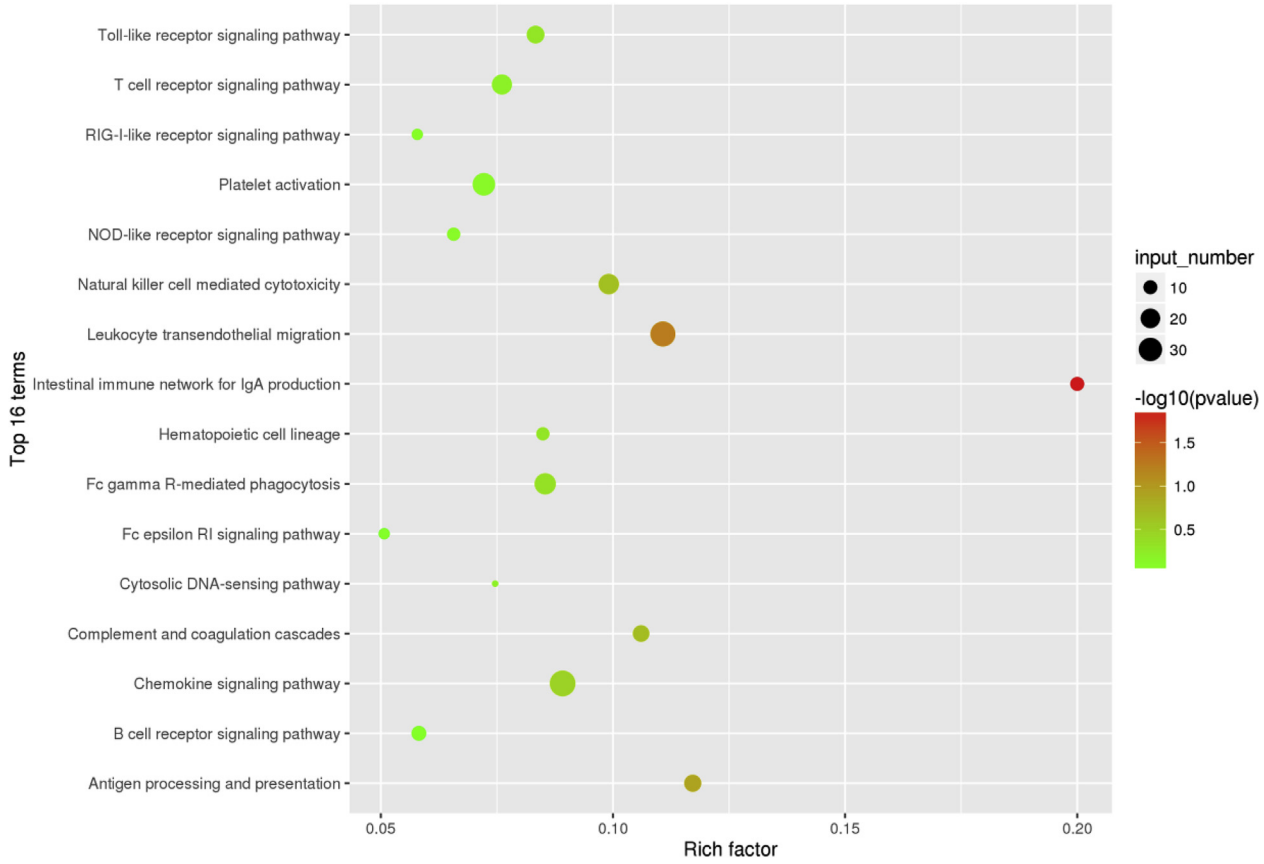

Fig. 4. Bubble graph of the top enrichment KEGG immune-related pathway. The red bubble is a remarkable pathway (adj p-value < 0.05); the biggest bubble with the brown colour is the pathway with the most differentially expressed genes and has the higher ratio; green bubbles are other pathways. (For interpretation of the references to colour in this figure legend, the reader is referred to the Web version of this article.)

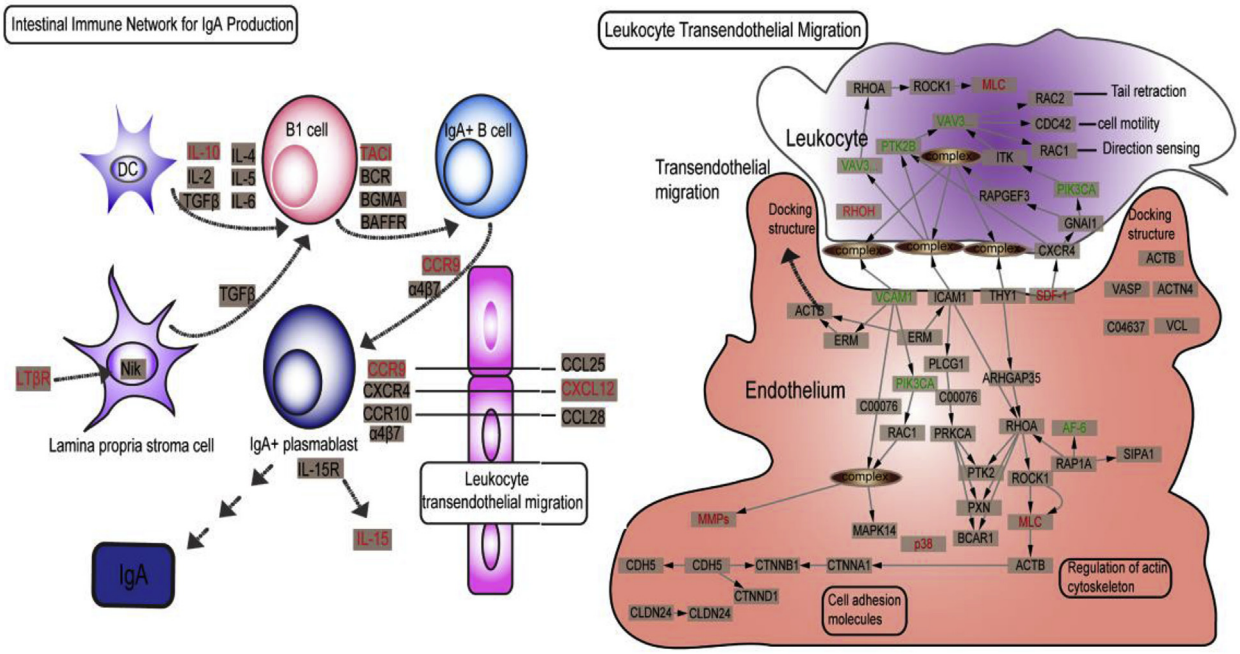

Fig. 5. Two of the top enrichment KEGG immune-related pathways. (a): relative expression levels of genes in the intestinal immune network for the IgA pathway. (b): relative expression levels of genes in the leukocyte transendothelial migration pathway. The black lettered genes in Fig. 5 are not differentially expressed, the red lettered genes in (a) and (b) are upregulated in spleens infected with the *RK21_RS10315*-RNAi strain compared with those infected with the wild-type strain, and the green lettered genes in (b) are downregulated in spleens infected with the *RK21_RS10315*-RNAi strain compared with those infected with the wild-type strain. (For interpretation of the references to colour in this figure legend, the reader is referred to the Web version of this article.)

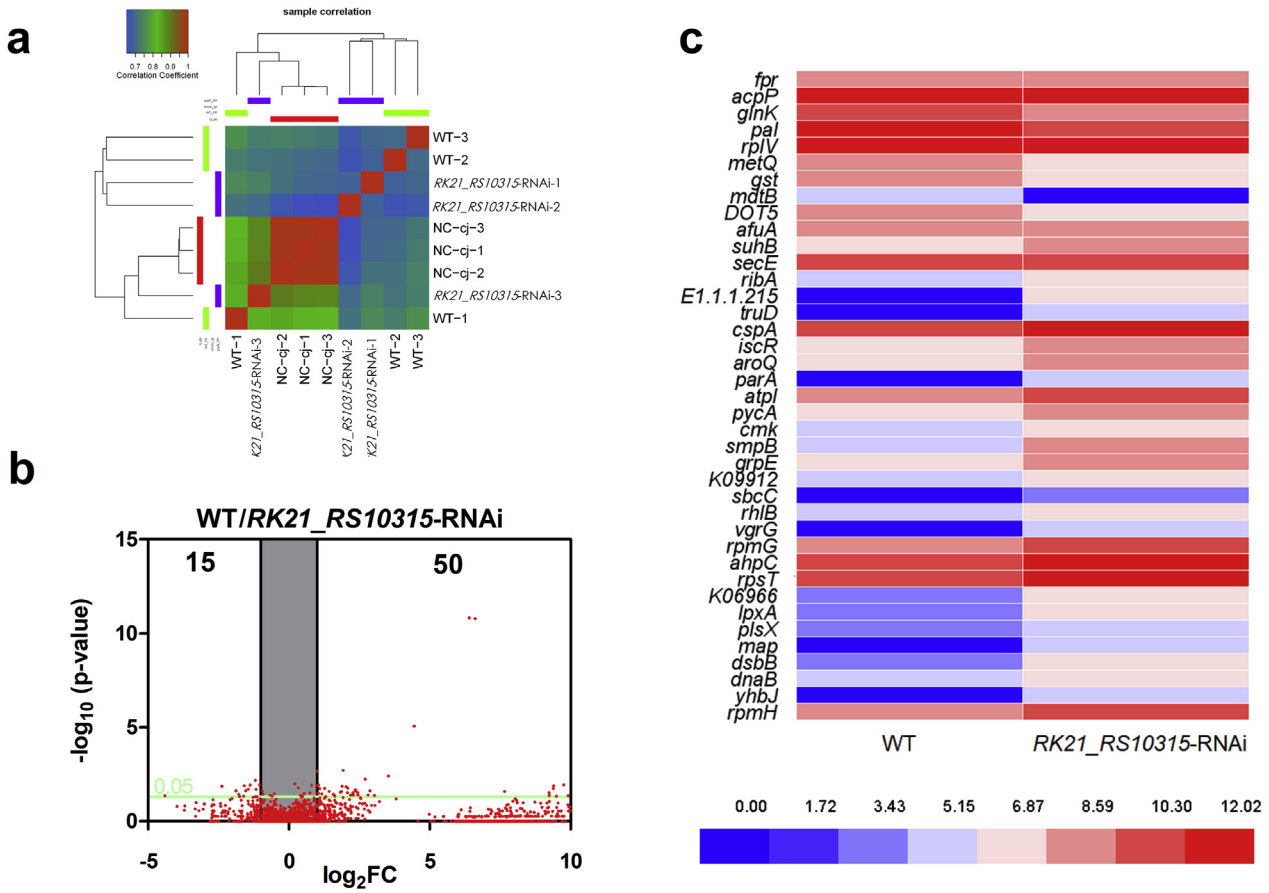

Fig. 6. Comparative transcriptional analysis of the pathogen infecting *E. coioides* spleens. (a): Reproducibility of transcriptional data (Pearson correlation coefficient (r) > 0.9). (b): Volcano plot obtained from *edgeR* analysis of infected *E. coioides* RNA pools. (c): Heat map of all the up- and downregulated genes from the pathogen transcripts (FDR < 0.05, $|\log_2 FC| \geq 1$). Colour-coding is based on $\log_2$FPKM (per kilobase of exon model per million mapped reads). (For interpretation of the references to colour in this figure legend, the reader is referred to the Web version of this article.)

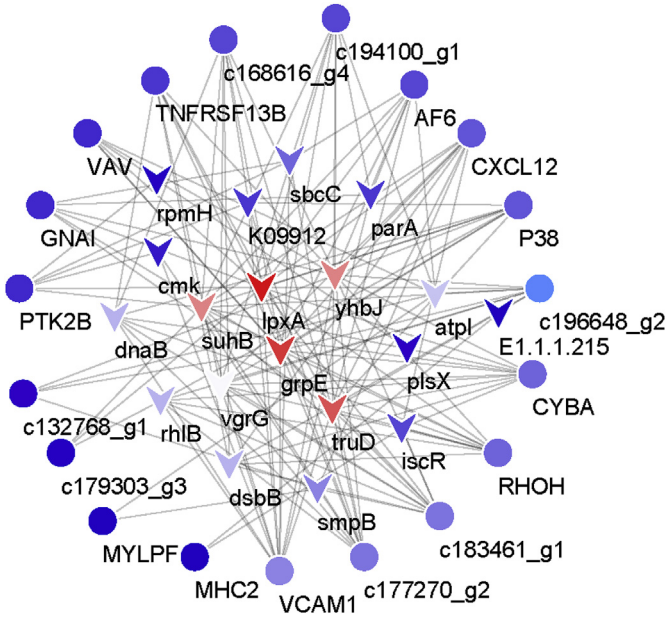

Fig. 7. The interaction relationships among the host differentially expressed genes from immune-related pathways and the pathogenic genes from DEMs. The redder the colour is, the greater the number of genes that were associated. (For interpretation of the references to colour in this figure legend, the reader is referred to the Web version of this article.)

studies.

Conflicts of interest

The authors declare that the research was conducted in the absence of any commercial or financial relationships that could be construed as a potential conflict of interest.

Acknowledgments

This work was supported by the Science and Technology Major/Special Project of Fujian Province under Contract No. 2016NZ0001-3, the Natural Science Foundation of Fujian Province under Contract No. 2016J05080.

Appendix A. Supplementary data

Supplementary data to this article can be found online at https://doi.org/10.1016/j.fsi.2019.02.025.

References

[1] Y. Sun, G. Luo, L. Zhao, et al., Integration of rnai and rna-seq reveals the immune responses of *Epinephelus coioides* to *sigX* gene of *Pseudomonas plecoglossicida*, Front. Immunol. 9 (2018) 1624 https://doi.org/10.3389/fimmu.2018.01624.
[2] B. Zhang, G. Luo, L. Zhao, L. Huang, Y. Qin, Y. Su, Q. Yan, Integration of RNAi and RNA-seq uncovers the immune responses of *Epinephelus coioides* to *L321_RS19110* gene of *Pseudomonas plecoglossicida*, Fish Shellfish Immunol. 81 (2018) 121–129 https://doi.org/10.1016/j.fsi.2018.06.051.
[3] A.M. Nuss, M. Beckstette, M. Pimenova, C. Schmühl, W. Opitz, F. Pisano,

A.K. Heroven, P. Dersch, Tissue dual RNA-seq allows fast discovery of infection-specific functions and riboregulators shaping host-pathogen transcriptomes, Proc. Natl. Acad. 114 (5) (2017) E791–E800 https://doi.org/10.1073/pnas.1613405114.
[4] A.J. Westermann, S.A. Gorski, J. Vogel, Dual RNA-seq of pathogen and host, Nat. Rev. Microbiol. 10 (9) (2012) 618–630 https://doi.org/10.1038/nrmicro2852.
[5] A.J. Westermann, K.U. Förstner, F. Amman, L. Barquist, Y. Chao, L.N. Schulte, L. Müller, R. Reinhardt, P.F. Stadler, J. Vogel, Dual RNA-seq unveils noncoding RNA functions in host-pathogen interactions, Nature 529 (7587) (2016) 496–501 https://doi.org/10.1038/nature16547.
[6] R. Aprianto, J. Slager, S. Holsappel, et al., Time-resolved dual RNA-seq reveals extensive rewiring of lung epithelial and pneumococcal transcriptomes during early infection, Genome Biol. 17 (2016) 198 https://doi.org/10.1186/s13059-016-1054-5.
[7] J. Hu, F. Zhang, X. Xu, et al., Isolation, identification and virulence of the pathogen of white-spots disease in internal organs of *Pseudosciaena crocea*, Oceanol. Limnol. Sinica 45 (2014) 409–417 https://doi.org/CNKI:SUN:HYFZ.0.2014-02-028.
[8] L. Huang, W. Liu, Q. Jiang, et al., Integration of transcriptomic and proteomic approaches reveals the temperature-dependent virulence of *Pseudomonas plecoglossicida*, Font. Cell. Infect. Microbiol. 8 (2018) 207 https://doi.org/10.3389/fcimb.2018.00207.
[9] J. Schumacher, X. Zhang, S. Jones, P. Bordes, M. Buck, ATP-dependent transcriptional activation by bacterial *PspF* AAA+protein, J. Mol. Biol. 338 (5) (2004) 863–875 https://doi.org/10.1016/j.jmb.2004.02.071.
[10] M. Bush, R. Dixon, The role of bacterial enhancer binding proteins as specialized activators of σ54-dependent transcription, Microbiol. Mol. Biol. Rev. 76 (3) (2012) 497–529 https://doi.org/10.1128/MMBR.00006-12.
[11] R.R. Burgess, A.A. Travers, J.J. Dunn, E.K.F. Bautz, Factor stimulating transcription by RNA polymerase, Nature 221 (5175) (1969) 43–46 https://doi.org/10.1038/221043a0.
[12] J.B. Stock, A.M. Stock, J.M. Mottonen, Signal transduction in bacteria, Nature 344 (6265) (1990) 395–400 https://doi.org/10.1038/344395a0.
[13] L.J. Reitzer, B. Magasanik, Transcription of *glnA* in E. coli is stimulated by activator bound to sites far from the promoter, Cell 45 (6) (1986) 785–792 https://doi.org/10.1016/0092-8674(86)90553-2.
[14] M. Buck, S. Miller, M. Drummond, R. Dixon, Upstream activator sequences are present in the promoters of nitrogen-fixation genes, Nature 320 (6060) (1986) 374–378 https://doi.org/10.1038/320374a0.
[15] M. Buck, M.T. Gallegos, D.J. Studholme, Y. Guo, J.D. Gralla, The Bacterial Enhancer-Dependent sigma 54 (sigma N) Transcription Factor, J. Bacteriol. 182 (15) (2000) 4129–4136 https://doi.org/10.1128/JB.182.15.4129-4136.2000.
[16] A. Wedel, S. Kustu, The bacterial enhancer-binding protein NtrC is a molecular machine: ATP hydrolysis is coupled to transcriptional activation, Genes Dev. 9 (16) (1995) 2042–2052 https://doi.org/10.1101/gad.9.16.2042.
[17] I. Rombel, A. North, I. Hwang, C. Wyman, S. Kustu, The bacterial enhancer-binding protein NtrC as a molecular machine, Cold Spring Harbor Symp. Quant. Biol. 63 (1998) 157–166 https://doi.org/10.1101/sqb.1998.63.157.
[18] D. Popham, D. Szeto, J. Keener, S. Kustu, Function of a bacterial activator protein that binds to transcriptional enhancers, Science 243 (4891) (1989) 629–635 https://doi.org/10.1126/science.2563595.
[19] G. Luo, L. Huang, Y. Su, et al., *flrA*, *flrB* and *flrC* regulate adhesion by controlling the expression of critical virulence genes in *Vibrio alginolyticus*, Emerg. Microb. Infect. 5 (2016) e85 https://doi.org/10.1038/emi.2016.82.
[20] L. Huang, Y. Zuo, Q. Jiang, et al., A metabolomic investigation into the temperature-dependent virulence of *Pseudomonas plecoglossicida* from large yellow croaker (*Pseudosciaena crocea*), J. Fish. Dis. 42 (3) (2019) 431–446 https://doi.org/10.1111/jfd.12957.
[21] K.J. Livak, T.D. Schmittgen, Analysis of relative gene expression data using real-time quantitative PCR and the $2^{-\Delta\Delta CT}$ method, Methods 25 (4) (2001) 402–408 https://doi.org/10.1006/meth.2001.1262.
[22] P.J.A. Cock, C.J. Fields, N. Goto, M.L. Heuer, P.M. Rice, The Sanger FASTQ file format for sequences with quality scores, and the Solexa/Illumina FASTQ variants, Nucleic Acids Res. 38 (6) (2010) 1767–1771 https://doi.org/10.1093/nar/gkp1137.
[23] Y. Erlich, P.P. Mitra, M. delaBastide, W.R. McCombie, G.J. Hannon, Alta-Cyclic: a self-optimizing base caller for next-generation sequencing, Nat. Methods 5 (8) (2008) 679–682 https://doi.org/10.1038/nmeth.1230.
[24] B. Langmead, S.L. Salzberg, Fast gapped-read alignment with Bowtie 2, Nat. Methods 9 (4) (2012) 357–359 https://doi.org/10.1038/NMETH.1923.
[25] M.G. Grabherr, B.J. Haas, M. Yassour, J.Z. Levin, D.A. Thompson, I. Amit, X. Adiconis, L. Fan, R. Raychowdhury, Q. Zeng, Z. Chen, E. Mauceli, N. Hacohen, A. Gnirke, N. Rhind, F. di Palma, B.W. Birren, C. Nusbaum, K. Lindblad-Toh, N. Friedman, A. Regev, Full-length transcriptome assembly from RNA-Seq data without a reference genome, Nat. Biotechnol. 29 (7) (2011) 644–652 https://doi.org/10.1038/nbt.1883.
[26] B. Li, C.N. Dewey, RSEM: accurate transcript quantification from RNA-Seq data with or without a reference genome, BMC Bioinf. 12 (2011) 323 https://doi.org/10.1186/1471-2105-12-323.
[27] M.D. Robinson, D.J. McCarthy, G.K. Smyth, edgeR: a Bioconductor package for differential expression analysis of digital gene expression data, Bioinformatics 26 (1) (2010) 139–140 https://doi.org/10.1093/bioinformatics/btp616.
[28] M. Kanehisa, S. Goto, KEGG: Kyoto Encyclopedia of Genes and Genomes, Nucleic Acids Res. 28 (1) (2000) 27–30 https://doi.org/10.1093/nar/28.1.27.
[29] C. Xie, X. Mao, J. Huang, Y. Ding, J. Wu, S. Dong, L. Kong, G. Gao, C.-Y. Li, L. Wei, KOBAS 2.0: a web server for annotation and identification of enriched pathways and diseases, Nucleic Acids Res. 39 (suppl_2) (2011) W316–W322 https://doi.org/10.1093/nar/gkr483.
[30] A. Beceiro, M. Tomás, G. Bou, Antimicrobial Resistance and Virulence: a Successful or Deleterious Association in the Bacterial World? Clin. Microbiol. Rev. 26 (2) (2013) 185–230 https://doi.org/10.1128/CMR.00059-12.
[31] Y. Qin, G. Lin, W. Chen, B. Huang, W. Huang, Q. Yan, Flagellar motility contributes to the invasion and survival of *Aeromonas hydrophila* in Anguilla japonica macrophages, Fish Shellfish Immunol. 39 (2) (2014) 273–279 https://doi.org/10.1016/j.fsi.2014.05.016.
[32] L. Guo, L. Huang, Y. Su, et al., *secA*, *secD*, *secF*, *yajC*, and *yidC* contribute to the adhesion regulation of *Vibrio alginolyticus*, Microbiologyopen (2017) e00551https://doi.org/10.1002/mbo3.551.
[33] W. Liu, L. Huang, Y. Su, et al., Contributions of the oligopeptide permeases in multistep of *Vibrio alginolyticus* pathogenesis, Microbiologyopen 6 (2017) e00511https://doi.org/10.1002/mbo3.511.
[34] D. Gu, M. Guo, M. Yang, et al., A σE-mediated temperature gauge controls a switch from LuxR-mediated virulence gene expression to thermal stress adaptation in *Vibrio alginolyticus*, PLoS Pathog. 12 (6) (2016) e1005645 https://doi.org/10.1371/journal.ppat.1005645.
[35] Z. Zhao, J. Liu, Y. Deng, W. Huang, C. Ren, D.R. Call, C. Hu, The *Vibrio alginolyticus* T3SS effectors, Val1686 and Val1680, induce cell rounding, apoptosis and lysis of fish epithelial cells, Virulence 9 (1) (2018) 318–330 https://doi.org/10.1080/21505594.2017.1414134.
[36] C. Wang, Y.L. Chen, W.P. Bian, S.-L. Xie, G.-L. Qi, L. Liu, P.R. Strauss, J.-X. Zou, D.-S. Pei, Deletion of *mstna* and *mstnb* impairs the immune system and affects growth performance in zebrafish, Fish Shellfish Immunol. 72 (2018) 572–580 https://doi.org/10.1016/j.fsi.2017.11.040.
[37] G.J. Hannon, RNA interference, Nature 418 (6894) (2002) 244–251 https://doi.org/10.1038/418244a.
[38] J. Moffat, D.A. Grueneberg, X. Yang, S.Y. Kim, A.M. Kloepfer, G. Hinkle, B. Piqani, T.M. Eisenhaure, B. Luo, J.K. Grenier, A.E. Carpenter, S.Y. Foo, S.A. Stewart, B.R. Stockwell, N. Hacohen, W.C. Hahn, E.S. Lander, D.M. Sabatini, D.E. Root, A lentiviral RNAi library for human and mouse genes applied to an arrayed viral high-content screen, Cell 124 (6) (2006) 1283–1298 https://doi.org/10.1016/j.cell.2006.01.040.
[39] Y. Qin, G. Lin, W. Chen, X. Xu, Q. Yan, Flagellar motility is necessary for *Aeromonas hydrophila* adhesion, Microb. Pathog. 98 (2016) 160–166 https://doi.org/10.1016/j.micpath.2016.07.006.
[40] L. Huang, L. Huang, Q. Yan, et al., The TCA Pathway is an Important Player in the Regulatory Network Governing *Vibrio alginolyticus* Adhesion Under Adversity, Front. Microbiol. 7 (40) (2016) 1–13 https://doi.org/10.3389/fmicb.2016.00040.
[41] Ø. Wessel, Ø. Haugland, M. Rode, B.N. Fredriksen, M.K. Dahle, E. Rimstad, Inactivated Piscine orthoreovirus vaccine protects against heart and skeletal muscle inflammation in Atlantic salmon, J. Fish. Dis. 41 (9) (2018) 1411–1419 https://doi.org/10.1111/jfd.12835.
[42] J. Liu, S.Y. Lu, L.H. Orfe, et al., ExsE Is a Negative Regulator for T3SS Gene Expression in *Vibrio alginolyticus*, Front. Cell. Infect. Microbiol. 6 (2016) 177 https://doi.org/10.3389/fcimb.2016.00177.
[43] X. Gao, H. Zhang, Q. Jiang, et al., Enterobacter cloacae associated with mass mortality in zoea of giant freshwater prawns *Macrobrachium rosenbergii* and control with specific chicken egg yolk immunoglobulins (IgY), Aquaculture 501 (2018) 331–337 https://doi.org/10.1016/j.aquaculture.2018.11.050.
[44] N. Chen, J. Jiang, X. Gao, X. Li, Y. Zhang, X. Liu, H. Yang, X. Bing, X. Zhang, Histopathological analysis and the immune related gene expression profiles of mandarin fish (Siniperca chuatsi) infected with Aeromonas hydrophila, Fish Shellfish Immunol. 83 (2018) 410–415 https://doi.org/10.1016/j.fsi.2018.09.023.
[45] B. Mi, G. Liu, W. Zhou, H. Lv, K. Zha, Y. Liu, Q. Wu, J. Liu, Bioinformatics analysis of fibroblasts exposed to tgf-β at the early proliferation phase of wound repair, Mol. Med. Rep. 16 (6) (2017) 8146–8154 https://doi.org/10.3892/mmr.2017.7619.
[46] K. Kiryluk, Y. Li, F. Scolari, S. Sanna-Cherchi, M. Choi, M. Verbitsky, D. Fasel, S. Lata, S. Prakash, S. Shapiro, C. Fischman, H.J. Snyder, G. Appel, C. Izzi, B.F. Viola, N. Dallera, L. Del Vecchio, C. Barlassina, E. Salvi, F.E. Bertinetto, A. Amoroso, S. Savoldi, M. Rocchietti, A. Amore, L. Peruzzi, R. Coppo, M. Salvadori, P. Ravani, R. Magistroni, G.M. Ghiggeri, G. Caridi, M. Bodria, F. Lugani, L. Allegri, M. Delsante, M. Maiorana, A. Magnano, G. Frasca, E. Boer, G. Boscutti, C. Ponticelli, R. Mignani, C. Marcantoni, D. Di Landro, D. Santoro, A. Pani, R. Polci, S. Feriozzi, S. Chicca, M. Galliani, M. Gigante, L. Gesualdo, P. Zamboli, G.G. Battaglia, M. Garozzo, D. Maixnerová, V. Tesar, F. Eitner, T. Rauen, J. Floege, T. Kovacs, J. Nagy, K. Mucha, L. Pączek, M. Zaniew, M. Mizerska-Wasiak, M. Roszkowska-Blaim, K. Pawlaczyk, D. Gale, J. Barratt, L. Thibaudin, F. Berthoux, G. Canaud, A. Boland, M. Metzger, U. Panzer, H. Suzuki, S. Goto, I. Narita, Y. Caliskan, J. Xie, P. Hou, N. Chen, H. Zhang, R.J. Wyatt, J. Novak, B.A. Julian, J. Feehally, B. Stengel, D. Cusi, R.P. Lifton, A.G. Gharavi, Discovery of new risk loci for IgA nephropathy implicates genes involved in immunity against intestinal pathogens, Nat. Genet. 46 (11) (2014) 1187–1196 https://doi.org/10.1038/ng.3118.
[47] L. Jostins, S. Ripke, R.K. Weersma, et al., Host–microbe interactions have shaped the genetic architecture of inflammatory bowel disease, Nature 491 (2012) 119 https://doi.org/10.1038/nature11582.
[48] R.C. Ferreira, Q. Pan-Hammarström, R.R. Graham, V. Gateva, G. Fontán, A.T. Lee, W. Ortmann, E. Urcelay, M. Fernández-Arquero, C. Núñez, G. Jorgensen, B.R. Ludviksson, S. Koskinen, K. Haimila, H.F. Clark, L. Klareskog, P.K. Gregersen, T.W. Behrens, L. Hammarström, Association of IFIH1 and other autoimmunity risk alleles with selective IgA deficiency, Nat. Genet. 42 (9) (2010) 777–780 https://doi.org/10.1038/ng.644.
[49] W.A. Muller, Mechanisms of leukocyte transendothelial migration, Annu. Rev. Pathol. 6 (1) (2011) 323–344 https://doi.org/10.1146/annurev-pathol-011110-130224.
[50] M.J. Allingham, J.D. Van Buul, K. Burridge, ICAM-1-mediated, Src-and Pyk2-

dependent vascular endothelial cadherin tyrosine phosphorylation is required for leukocyte transendothelial migration, J. Immunol. 179 (6) (2007) 4053–4064 https://doi.org/10.4049/jimmunol.179.6.4053.
[51] W.A. Muller, S.A. Weigl, X. Deng, et al., PECAM-1 is required for transendothelial migration of leukocytes, J. Exp. Med. 178 (2) (1993) 449–460 https://doi.org/10.1084/jem.178.2.449.
[52] R.A. Worthylake, K. Burridge, Leukocyte transendothelial migration: orchestrating the underlying molecular machinery, Curr. Opin. Cell Biol. 13 (5) (2001) 569–577 https://doi.org/10.1016/S0955-0674(00)00253-2.
[53] S. Schulze, J. Schleicher, R. Guthke, et al., How to Predict Molecular Interactions between Species? Front. Microbiol. 7 (2016) 442 https://doi.org/10.3389/fmicb.2016.00442.
[54] J. Parkin, B. Cohen, An overview of the immune system, Lancet 357 (9270) (2001) 1777–1789 https://doi.org/10.1016/S0140-6736(00)04904-7.
[55] K. Ganeshan, A. Chawla, Metabolic regulation of immune responses, Annu. Rev. Immunol. 32 (1) (2014) 609–634 https://doi.org/10.1146/annurev-immunol-032713-120236.